



Effects of Replacing Thiophene with 5,5-Dimethylcyclopentadiene in Alternating Poly(phenylene), Poly(3-hexylthiophene), and Poly(fluorene) Copolymer Derivatives

Journal:	<i>Polymer Chemistry</i>
Manuscript ID	PY-ART-08-2015-001247.R1
Article Type:	Paper
Date Submitted by the Author:	01-Sep-2015
Complete List of Authors:	Chen, Lei; Rutgers University, Chemistry Wang, Karen; Rutgers University, Chemistry Mahmoud, Sufian; Rutgers University, Chemistry Li, Yuan; Wake Forest, Center for Nanotechnology and Molecular Materials, Department of Physics Huang, Huihui; Wake Forest, Center for Nanotechnology and Molecular Materials, Department of Physics Huang, Wenxiao; Wake Forest, Center for Nanotechnology and Molecular Materials, Department of Physics Xu, Junwei; Wake Forest, Center for Nanotechnology and Molecular Materials, Department of Physics Dun, Chaochao; Wake Forest, Center for Nanotechnology and Molecular Materials, Department of Physics Carroll, Dave; Wake Forest University, Department of Physics Pietrangelo, Agostino; Rutgers University, Department of Chemistry



Effects of Replacing Thiophene with 5,5-Dimethylcyclopentadiene in Alternating Poly(phenylene), Poly(3-hexylthiophene), and Poly(fluorene) Copolymer Derivatives†

Received 00th January 20xx,
Accepted 00th January 20xx

DOI: 10.1039/x0xx00000x

www.rsc.org/

L. Chen,^a K. Wang,^a S. M. Mahmoud,^a Y. Li,^b H. Huang,^b W. Huang,^b J. Xu,^b C. Dun,^b D. Carroll,^b and A. Pietrangelo*^a

Poly(phenylene), poly(3-hexylthiophene), and poly(fluorene)-based copolymers bearing alternating thiophene (PPT, P3HTT, and PFT) and 5,5-dimethylcyclopentadiene co-repeat units (PPCp, P3HTCp, PFCp) were examined to establish how the identity of the latter manipulates the optical absorption, photoluminescence, thermal properties, (spectro)electrochemistry, and atmospheric stability of these systems. The results of our investigation show that the 4 π electron diene moiety reduces the optical band gap of the poly(fluorene) and poly(3-hexylthiophene)-based copolymers when compared against their all-aromatic congeners while having the opposite effect on the poly(phenylene) class. Fluorescence studies reveal that the emission maxima λ_{em} of the diene systems are lower in energy among the three copolymer sets, however, quantum yields Φ_f are also lower indicating that the diene-moiety compromises photoluminescence. Regarding thermal properties, the identity of the co-repeat unit (*i.e.* diene vs thiophene) was found to have a negligible effect on copolymer glass-transition temperature T_g , however, the polyaromatics exhibit higher thermal stability irrespective of copolymer class. Cyclic voltammetry data show that the onset of oxidation (E_{onset}) decreases in the order of poly(fluorene), poly(phenylene), and poly(3-hexylthiophene) derivatives suggesting that the aromatic co-repeat units play a critical role in establishing the HOMO energy. Moreover, when copolymers within each class are compared, the diene-containing systems always exhibit a lower E_{onset} indicating that the diene moiety increases the HOMO energy when used in lieu of thiophene. Solution-phase stability studies under ambient atmospheric conditions show the poly(3-hexylthiophene)s to be the most stable class of copolymers followed by the poly(phenylene)s and poly(fluorene)s respectively. In addition to the comparative analyses described herein, three model configurational triads of the poly(3-hexylthiophene) derivative P3HTCp were characterized to allow for the unambiguous assignment of copolymer regiochemistry that was determined to be regiorandom. Finally, a polymer light-emitting diode (PLED) was constructed using PFCp as the emissive layer as a proof-of-principle that diene-containing copolymers can be used as active materials in opto-electronic devices.

Introduction

Thiophene is a frequently employed building block used in the production of π -conjugated (macro)molecules, a ubiquitous class of semiconducting materials studied extensively in the field of organic electronics.¹ The five-membered heterocycle consists of a sulfur atom and four sp²-hybridized carbon atoms that form a delocalized 6 π electron system, lending these materials their highly desirable optical and electronic properties, environmental stability, and structural versatility by way of functional group addition.² Recently, several studies have reported on the dearomatization of thiophene building

blocks into 4 π electron thiophene-1,1-dioxide derivatives,³ a chemical transformation that drastically affects the electronic structure of π -conjugated (macro)molecules by reducing their optical band gap, lowering frontier orbital energies (particularly the LUMO), and increasing electron affinity.⁴ These findings have triggered interest into the potential application of these systems as electron-transporting materials⁵ and active layers in third-generation solar devices that could increase efficiency beyond the Shockley-Queisser limit due to their ability to exhibit highly efficient intramolecular singlet fission.⁶

In light of these works, our group has been interested in examining how the properties of thiophene-based materials are manipulated when supplanting the heterocyclic moiety with 5,5-dimethylcyclopentadiene, another 4 π electron system that is isostructural to thiophene save for a geminal dimethyl group that is present in lieu of sulfur. Indeed, these nonaromatic building blocks offer the ability to reduce the overall aromaticity of the material without significantly

^a Department of Chemistry, Rutgers University-Newark, 73 Warren Street, Newark, New Jersey 07102, USA. E-mail: a.pietrangelo@rutgers.edu

^b Center for Nanotechnology and Molecular Materials, Department of Physics, Wake Forest, Winston-Salem, NC 27109, USA

† Electronic Supplementary Information (ESI) available: Characterization data including NMR spectra (¹H, HSQC, HMBC), DSC/TGA thermograms, fluorescence data, and cyclic voltammograms. See DOI: 10.1039/x0xx00000x

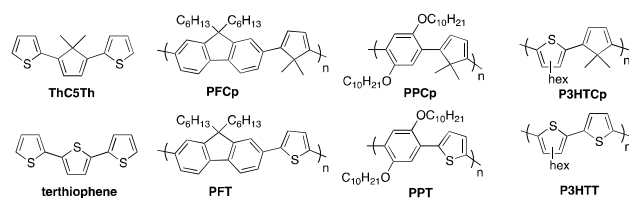


Chart 1

affecting its topology and hole-conducting capability, all the while promoting polyene-like quinoid formation that is necessary for charge-carrier delocalization upon doping.⁷ Towards this end, we recently reported on an efficient route to a series of cyclopentadiene-containing π -conjugated triads including the terthiophene derivative ThC5Th (Chart 1).⁸ Single-crystal X-ray crystallographic studies revealed that dihedral angles between adjacent rings lie in the range of *ca.* 0–18° indicating that the geminal dimethyl groups do not compromise the planarity of the systems. Moreover, a comparative analysis with terthiophene indicate that the diene-moiety reduces the HOMO-LUMO energy gap of the system while increasing the energy of the HOMO orbital, a trend that was also observed when comparing electrochemically generated (co)polymer films prepared from these two systems.⁹ In an independent study, Breslow and coworkers have shown that substituting thiophene with 5,5-dimethylcyclopentadiene can also improve single-molecule junction conductance in molecular wires, an effect that has been attributed to a reduction in aromatic stabilization that arises from the diene scaffold.¹⁰

The objective of the present study is two fold: first, to examine how the optical and electronic properties of a π -conjugated copolymer class is influenced when replacing alternating thienyl constituents with 5,5-dimethylcyclopentadienes and second, to evaluate how these influences compare among copolymer classes as a function of comonomer identity. Specifically, we outline the synthesis and characterization of alternating poly(phenylene) and poly(3-hexylthiophene) derivatives (**PPT**, **PPCp**, **P3HTT**, and **P3HTCp**, Chart 1) as they represent common copolymer architectures that are well established in the literature. Their properties are then compared to those of poly(flourene) derivatives (**PFT** and **PFCp**, Chart 1) recently published by our group.⁸ We also report on the fabrication and performance of a polymer light-emitting diode (PLED) using **PFCp** as the emissive layer which to the best of our knowledge is the first example of any kind of (opto)electronic device to employ a cyclopentadiene-based polymer as an active layer. Ultimately, the results described herein provide a foundation for future efforts that will focus on utilizing polyene-like π -conjugated systems as active materials in (opto)electronic devices with targeted properties and potentially enhanced performances.

Experimental

Materials and Equipment

All reactions were performed under a dinitrogen atmosphere using standard Schlenk techniques unless otherwise noted. Anhydrous solvents (tetrahydrofuran (THF), toluene (tol), and dichloromethane (DCM)) were dried and collected from a PureSolv MD solvent purification system (Innovative Technology, Inc.) equipped with two activated alumina columns. All reagents were purchased from Sigma Aldrich or VWR and used as received unless otherwise noted. **PFT**, **PFCp**,⁸ 2,5-didecyloxyphenylene-1,4-bis(4,4,5,5-tetramethyl-1,3,2-dioxaborolane)¹¹ and 3-hexylthiophene-bis(4,4,5,5-tetramethyl-1,3,2-dioxaborolane)¹² were prepared according to procedures published elsewhere. Indium Tin Oxide (ITO) deposited on glass (resistivity, 4–10 Ω) was purchased from Delta Technologies Ltd. Tetrabutylammonium hexafluorophosphate (TBAPF₆) was recrystallized from absolute ethanol (3x) and dried *in vacuo* prior to use. Chromatographic purification was conducted on silica gel (60 Å porosity, SORBTECH) or neutral alumina (58 Å porosity, Sigma Aldrich). UV/vis spectra were recorded on a Cary-100 spectrophotometer. Molecular weights (M_n and M_w) and dispersity (D_M) were determined by gel-permeation chromatography (GPC) using a Malvern Viscotek TDAmx chromatograph with THF as the mobile phase at 30°C. The chromatograph was equipped with two PLC mixed columns and one PLD mixed column. Output was detected with a Viscotek TDA 305-055 Tetra Detector Array (PDA+RI+Visc+LALS/RALS) using an eluent flow rate of 1 mL/min and a 60 μ L injection loop. Molecular weights were determined from a 10-point calibration curve created using poly(styrene) standards purchased from Polymer Laboratories. Matrix-assisted laser desorption/ionization time-of-flight (MALDI-TOF) mass spectrometry was performed on a Bruker ultrafleXtreme MALDI-TOF analyzer. Anthracene (or 2,5-dihydroxybenzoic acid) and myoglobin were used as the matrix and calibration internal standard respectively. Excitation and emission spectra were measured on a Varian Cary Eclipse fluorescence spectrophotometer. Absolute quantum yields (Φ_F) were determined using a HORIBA Jobin Yvon Fluorolog spectrofluorimeter equipped with a Quanta- ϕ calibrated integrating sphere system. GC-MS measurements were conducted on an Agilent Technologies HP6890 GC system and 5973A MSD. The standard method involved an initial oven temperature of 70°C (held for 1 min) followed by a 10°C min⁻¹ ramp to 250°C. Copolymer thin films were prepared by spin-coating THF solutions (*ca.* 5 mg/mL) onto glass substrates or by drop-casting. Thermal gravimetric analyses (TGA) were performed on a TA Instruments Discovery thermogravimetric analyzer at a heating rate of 20°C min⁻¹ to 700°C. Differential scanning calorimetry (DSC) was performed on a TA Instruments Discovery differential calorimeter at a scan rate of 10°C min⁻¹ from *ca.* -40°C to 170°C. Glass transition temperatures were obtained from the second heating curves. ¹H NMR spectra were recorded on a Bruker Ascend 500 MHz spectrometer and calibrated to the residual protonated

solvent peak at δ 7.24 for deuterated chloroform (CDCl_3) and δ 5.32 for deuterated dichloromethane (CD_2Cl_2). ^{13}C NMR spectra were calibrated at δ 77.2 for CDCl_3 and δ 54.0 for CD_2Cl_2 . Cyclic voltammetry experiments were conducted with the use of a Metrohm AUTOLAB PGSTAT302N potentiostat/galvanostat. All experiments were performed in a single compartment cell using a platinum disk (*ca.* 3 mm²) working electrode, platinum mesh counter electrode, and quasi-silver wire reference electrode at a scan rate of 100 mV/s. Electrochemical solutions were composed of anhydrous TBAPF₆ (0.1 M) and copolymer (*ca.* 5.6 mM) in anhydrous DCM. Decamethylferrocene (Fc^*Cp^*_2) was used as an internal standard.

Spectroelectrochemistry

A copolymer modified ITO working electrode, platinum mesh counter electrode, and silver foil reference electrode were placed in a quartz cuvette, which was charged with electrolyte solution (TBAPF₆, 0.1 M in anhydrous acetonitrile, MeCN) and loaded into a UV/vis-NIR spectrophotometer. The working electrode was oxidized at a fixed potential for 180 s, during which time an optical absorption spectrum was taken. The film was then reduced back to its neutral state and a second absorption spectrum taken to ensure that no damage to the film had occurred prior to subsequent experiments. The process was repeated at progressively higher positive potentials.

Solution-phase Degradation Studies

Analyte solutions were prepared ((1-10) 10⁻⁴ M) in 100 mL volumetric flasks using DCM as solvent. Each solution was then portioned into seven 10 mL volumetric flasks and left exposed to ambient light and atmosphere.¹³ Over the course of several hours, UV/vis absorption measurements were taken periodically and λ_{max} recorded as a function of time.

PPCp. A Schlenk flask was charged with potassium fluoride, KF (383 mg, 6.6 mmol) and deionized water (*ca.* 2 mL) and the solution sparged with dinitrogen for 10 minutes. To this flask, a comonomer solution comprised of 2,5-didicyloxyphenylene-1,4-bis(4,4,5,5-tetramethyl-1,3,2-dioxaborolane) (642 mg, 1 mmol) and 5,5-dimethyl-1,4-bis(trifluoromethanesulfonyl)-1,3-cyclopentadiene **1**, (390 mg, 1 mmol) in *ca.* 5 mL of deoxygenated THF was added followed by a catalyst solution of bis(dibenzylideneacetone) palladium (0), Pd(dba)₂ (46 mg, 0.08 mmol) and tricyclohexylphosphine, P(Cy)₃ (27 mg, 0.096 mmol) in *ca.* 5 mL of deoxygenated toluene. After stirring for 72 h at room temperature, the brown mixture was diluted with deionized water (*ca.* 30 mL) and the organics extracted with DCM (3x *ca.* 100 mL). The organic phases were collected, washed with brine (2x *ca.* 20 mL), and dried over anhydrous magnesium sulfate, MgSO₄. After filtration, the solvent was removed by reduced pressure to afford a red solid that was dissolved in *ca.* 3 mL of THF and precipitated in cold methanol (*ca.* 100 mL at 0°C) to afford 278 mg of a black powder (Yield 58%). ^1H NMR (CD_2Cl_2 , 500 MHz): δ 6.96 (1H, s), 6.77 (1H, s),

3.97 (2H, t), 1.79 (2H, m), 1.20-1.50 (17H, m), 0.88 (3H, t). UV-vis (CH_2Cl_2): λ_{max} (ϵ): = 365 (8400) nm ($\text{L mol}^{-1} \text{cm}^{-1}$). Emission @ 550 nm and excitation @ 458 nm. Φ_{F} = 18±4%.

PPT. A Schlenk flask was charged with tetrabutylammonium bromide, TBAB (36 mg, 0.102 mmol), potassium carbonate, K₂CO₃ (287 mg, 2.07 mmol) and deionized water (*ca.* 2 mL) and the solution sparged with dinitrogen gas for 10 min. A comonomer solution comprised of 2,5-didicyloxyphenylene-1,4-bis(4,4,5,5-tetramethyl-1,3,2-dioxaborolane) (460 mg, 0.716 mmol) and 2,5-diiodothiophene (241 mg, 0.716 mmol) in *ca.* 5 mL of deoxygenated THF was added to the flask followed by a catalyst solution of tetrakis(triphenylphosphine) palladium(0), Pd(PPh₃)₄ (0.043 g, 0.04 mmol) in *ca.* 3 mL of deoxygenated toluene. After degassing the mixture (freeze-pump-thaw, 3x), the flask was placed in an oil bath with stirring at 100°C for 72 h. The red mixture was diluted with deionized water (*ca.* 30 mL) and the organics extracted with DCM (3x *ca.* 100 mL). The organic phases were collected, washed with brine (2x *ca.* 20 mL), and dried over anhydrous MgSO₄. After filtration, the solvent was removed by reduced pressure to afford a dark red solid that was dissolved in *ca.* 3 mL of THF and precipitated in cold methanol (*ca.* 100 mL at 0°C). The solid was redissolved in THF and precipitated in cold hexanes (*ca.* 100 mL at 0°C) to afford 220 mg (Yield 65%) of dark red powder. ^1H NMR (CD_2Cl_2 , 500 MHz): δ 7.61(2H, s), 7.35 (2H, s), 4.17 (4H, s), 1.97 (3H, s), 1.58 (3H, s), 1.10-1.45 (26H, m), 0.87 (6H, m). UV-vis (CH_2Cl_2): λ_{max} (ϵ): = 454 (23300) nm ($\text{L mol}^{-1} \text{cm}^{-1}$). Emission @ 517 nm and excitation @ 458 nm. Φ_{F} = 48±7%.

P3HTCp. A Schlenk flask was charged with KF (255 mg, 4.389 mmol) and deionized water (*ca.* 1 mL) and the solution sparged with dinitrogen for 10 minutes. A comonomer solution of 3-hexylthiophene-bis(4,4,5,5-tetramethyl-1,3,2-dioxaborolane) (280 mg, 0.667 mmol) and **1** (260 mg, 0.667 mmol) in *ca.* 4 mL of deoxygenated THF was added to the flask followed by a catalyst solution of Pd(dba)₂ (39 mg, 0.067 mmol) and P(Cy)₃ (74 mg, 0.267 mmol) in *ca.* 4 mL of deoxygenated toluene. After stirring for 72 h at room temperature, the red mixture was diluted with deionized water (*ca.* 30 mL) and the organics extracted with DCM (3x *ca.* 100 mL). The organic phases were collected, washed with brine (2x *ca.* 20 mL), and dried over anhydrous MgSO₄. After filtration, the solvent was removed by reduced pressure to afford a red solid that was dissolved in *ca.* 3 mL of THF and precipitated in cold methanol (*ca.* 100 mL at 0°C) to afford 81 mg (Yield 47%) of black powder. ^1H NMR (CD_2Cl_2 , 500 MHz): δ 6.40-7.23 (3H, m), 2.58-2.90 (2H, m), 1.32-1.72 (14H, m), 0.91 (3H, s). UV-vis (CH_2Cl_2): λ_{max} (ϵ): = 476 (9200) nm ($\text{L mol}^{-1} \text{cm}^{-1}$). Emission @ 600 nm and excitation @ 300 nm. Φ_{F} = 5±3%.

P3HTT. A Schlenk flask was charged with TBAB (36 mg, 0.102 mmol), K₂CO₃ (287 mg, 2.07 mmol) and deionized water (*ca.* 2 mL) and the solution sparged with dinitrogen gas for 10 min. A comonomer solution of 3-hexylthiophene-bis(4,4,5,5-tetramethyl-1,3,2-dioxaborolane) (301 mg, 0.716 mmol) and

2,5-diiodothiophene (241 mg, 0.716 mmol) in *ca.* 5 mL of deoxygenated THF was added to the flask followed by a catalyst solution of Pd(PPh₃)₄ (43 mg, 0.04 mmol) in *ca.* 3 mL of deoxygenated toluene. After degassing the mixture (freeze-pump-thaw, 3x), the flask was placed in an oil bath with stirring at 100 °C for 72 h. The red mixture was then diluted with deionized water (*ca.* 30 mL) and the organics extracted with DCM (3x *ca.* 100 mL). The organic phases were collected, washed with brine (2x *ca.* 20 mL), and dried over anhydrous MgSO₄. After filtration, the solvent was removed by reduced pressure to afford a dark red solid that was dissolved in *ca.* 3 mL of THF and precipitated in cold methanol (*ca.* 100 mL at 0°C). Once isolated, the solid was redissolved in THF and precipitated in 100 mL hexanes to afford 72 mg (Yield 41%) of dark red powder. ¹H NMR (CD₂Cl₂, 500 MHz): δ 6.80-7.80 (3H, m), 3.20-3.70 (1H, m), 2.50-2.90 (1H, m), 1.00-1.80 (8H, m), 0.90 (3H, s). UV-vis (CH₂Cl₂): λ_{max} (ε) = 456 (17500) nm (L mol⁻¹ cm⁻¹). Emission @ 563 nm and excitation @ 456 nm. Φ_F = 35±7%.

Compound 3. A Schlenk flask was charged with KF (380 mg, 6.6 mmol), deionized water (*ca.* 1 mL), and the solution sparged with dinitrogen for 10 minutes. Comonomers 5,5-dimethyl-1,4-bis(trifluoromethanesulfonyl)-1,3-cyclopentadiene (390 mg, 1 mmol) and 4-hexylthiophene-2-boronic acid pinacol ester (650 mg, 2.2 mmol) in *ca.* 4 mL of deoxygenated THF were then added followed by a catalyst solution of Pd(dba)₂ (46 mg, 0.08 mmol) and P(Cy)₃ (27 mg, 0.096 mmol) in *ca.* 3 mL of deoxygenated THF. After stirring at room temperature for 24 h, the solution was diluted with water (*ca.* 20 mL) and the organics extracted with DCM (3x *ca.* 30 mL). The organic phases were collected and washed with brine (2x *ca.* 20 mL) and dried over anhydrous MgSO₄. After removing the solvent, the crude product was purified by flash chromatography on neutral alumina using hexanes as the eluent (*R_f* = 0.84). The product was isolated as a yellow oil (366 mg, Yield 86%). ¹H NMR (CD₂Cl₂, 500 MHz): δ 7.01 (1H, s), 6.80 (1H, s), 6.65 (1H, s), 2.60 (2H, t), 1.64 (2H, m), 1.28-1.55 (9H, m), 0.90 (3H, t). ¹³C NMR (CD₂Cl₂, 100 MHz): δ 151.73, 144.52, 139.14, 125.20, 124.78, 118.71, 54.29, 32.27, 31.07, 31.04, 29.62, 24.88, 23.22, 14.44. UV-vis (CH₂Cl₂): λ_{max} (ε) = 391 (15000) nm (L mol⁻¹ cm⁻¹). Emission @ 465 nm and excitation @ 391 nm. GC/MS: *m/z* (%): 426 (100%) [M+], 281 (9%), 253 (5%), 207 (25%), 143 (6%).

Compound 4. A Schlenk flask was charged with KF (380 mg, 6.6 mmol) and deionized water (*ca.* 1 mL) and the solution sparged with dinitrogen for 10 minutes. Comonomers 5,5-dimethyl-1,4-bis(trifluoromethanesulfonyl)-1,3-cyclopentadiene (390 mg, 1 mmol) and 3-hexylthiophene-2-boronic acid pinacol ester (650 mg, 2.2 mmol) in *ca.* 4 mL of deoxygenated THF were then added followed by a catalyst solution of Pd(dba)₂ (46 mg, 0.08 mmol) and P(Cy)₃ (27 mg, 0.096 mmol) in *ca.* 3 mL of deoxygenated THF. After stirring at room temperature for 24 h, the solution was diluted with water (*ca.* 20 mL) and the organics extracted with DCM (3x *ca.* 30 mL). The organic phases were collected and washed with brine (2x *ca.* 20 mL) and dried over anhydrous MgSO₄. After

removing the solvent, the crude product was purified by flash chromatography on neutral alumina using hexanes as the eluent (*R_f* = 0.80). The product was isolated as a yellow oil (360 mg, Yield 85%). ¹H NMR (CD₂Cl₂, 500 MHz): δ 7.25 (1H, d), 7.01 (1H, d), 6.46 (1H, s), 2.63 (2H, t), 1.61 (2H, m), 1.26-1.41 (9H, m), 0.89 (3H, t). ¹³C NMR (CD₂Cl₂, 100 MHz): δ 150.58, 141.67, 132.52, 129.49, 129.27, 123.73, 56.87, 32.31, 31.66, 30.03, 29.87, 23.22, 22.39, 14.44. UV-vis (CH₂Cl₂): λ_{max} (ε) = 336 (15290) nm (L mol⁻¹ cm⁻¹). Emission @ 452 nm and excitation @ 337 nm. GC/MS: *m/z* (%): 426 (100%) [M+], 341 (7%), 221 (6%), 163 (13%), 135 (5%).

Compound 5. A Schlenk flask was charged with KF (190 mg, 3.3 mmol) and deionized water (*ca.* 1 mL) and the solution sparged with dinitrogen for 10 minutes. Comonomers 5,5-dimethyl-1,4-bis(trifluoromethanesulfonyl)-1,3-cyclopentadiene (390 mg, 1 mmol) and 3-hexylthiophene-2-boronic acid pinacol ester (330 mg, 1.1 mmol) in *ca.* 3 mL of deoxygenated THF were then added followed by a catalyst solution of Pd(dba)₂ (23 mg, 0.04 mmol) and P(Cy)₃ (14 mg, 0.05 mmol) in *ca.* 2 mL of deoxygenated THF. After stirring at room temperature for 3 h, the solution was diluted with water (*ca.* 10 mL) and the organics extracted with DCM (3x *ca.* 10 mL). The organic phases were collected and washed with brine (2x *ca.* 10 mL) and dried over anhydrous MgSO₄. After removing the solvent, the crude product was purified by flash chromatography on neutral alumina using hexanes as the eluent (*R_f* = 0.28). The mono-coupled intermediate product was isolated as an unstable light purple oil (180 mg, 44%) that was used immediately without further purification. ¹H NMR (CD₂Cl₂, 500 MHz): δ 7.25 (1H, d), 7.00 (1H, d), 6.26 (1H, d), 6.20 (1H, d), 2.58 (2H, t), 1.50-1.59 (4H, m), 1.27-1.31 (10H, m), 0.88 (3H, t). ¹³C NMR (CD₂Cl₂, 100 MHz): δ 160.49, 144.94, 142.63, 130.79, 129.62, 125.80, 124.27, 117.91, 113.19, 52.69, 32.25, 31.58, 29.85, 29.78, 23.17, 20.79, 14.39, 11.76.

A Schlenk flask was charged with KF (65 mg, 1.121 mmol) and deionized water (*ca.* 1 mL) and the solution was sparged with dinitrogen for 10 minutes. A comonomer solution comprised of the mono-coupled intermediate (70 mg, 0.172 mmol) and 4-hexylthiophene-2-boronic acid pinacol ester (76 mg, 0.256 mmol) in *ca.* 2 mL of deoxygenated THF was added to the flask followed by a catalyst solution comprised of Pd(dba)₂ (10 mg, 0.017 mmol) and P(Cy)₃ (19 mg, 0.068 mmol) in *ca.* 3 mL of deoxygenated THF. After stirring for 24 h at room temperature, the yellow mixture was diluted with deionized water (*ca.* 5 mL) and the organics extracted with DCM (3x *ca.* 10 mL). The organic phases were collected and washed with brine (2x *ca.* 10 mL) and dried over anhydrous MgSO₄. After removing the solvent, the crude product was purified by flash chromatography on neutral alumina using hexanes as the eluent (*R_f* = 0.88). The product was isolated as a yellow oil (17 mg, Yield 23%). ¹H NMR (CD₂Cl₂, 500 MHz): δ 7.24 (1H, d), 7.00 (2H, d), 6.81 (1H, s), 6.69 (1H, d), 6.41 (1H, d), 2.60 (4H, t), 1.29-1.62 (22H, m), 0.82-0.96 (6H, m). ¹³C NMR (CD₂Cl₂, 100 MHz): δ 151.35, 150.86, 144.50, 141.90, 139.31, 132.22, 129.53, 129.39, 125.03, 124.95, 123.63, 118.70, 55.51, 32.27,

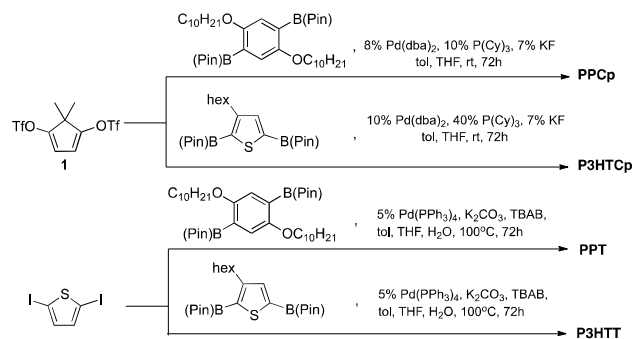
32.26, 31.61, 31.07, 31.03, 30.04, 29.85, 29.61, 23.53, 23.21, 23.19, 14.43, 14.40. UV-vis (CH_2Cl_2): λ_{max} (ϵ): = 363 (14326) nm ($\text{L mol}^{-1} \text{cm}^{-1}$). Emission @ 460 nm and excitation @ 355 nm. GC/MS: m/z (%): 426 (100%) [M^+], 355 (6%), 281 (13%), 253 (8%), 235 (5%), 207 (38%), 163 (6%), 135 (6%).

Results and discussion

Synthesis and Structural Characterization

All copolymers were prepared according to Scheme 1 using Suzuki-Miyaura polycondensation methods.¹⁴ Palladium-catalysed C-C cross-coupling between 5,5-dimethyl-1,4-bis(trifluoromethanesulfonyl)-1,3-cyclopentadiene **1** and the appropriate diboronic acid pinacol ester afforded copolymers **PPCp** and **P3HTCp** under ambient conditions. In contrast, the production of **PPT** and **P3HTT** required elevated temperatures (*ca.* 100 °C) to induce product formation. GPC traces (Figures S1-4) recorded with RI and PDA detectors are predominantly monomodal with dispersities in the range of 1.3-2.5. In line with its proposed structure, the ^1H NMR spectrum of **PPCp** possesses singlets at δ 6.77 and 6.96 ppm (Figures 1a and S5) that are consistent with the proton environments that comprise the π -conjugated components of the copolymer backbone, resonances that are also located up-field from those of **PPT** (*ca.* δ 7.35 and 7.61 ppm, Figure S6). In the case of **P3HTCp**, the spectroscopic features in the aromatic region are complex (Figures 1b and S7) as a result of copolymer regiochemistry that arises from the asymmetry of the 3-hexylthiophene units (to be discussed later). Nonetheless, the relative integral ratios of the linear aliphatic CH_3 protons and those of the diene moieties are 6:2 and 3:2 for **PPCp** and **P3HTCp** respectively, suggesting that molar equivalents of each comonomer repeat unit are present in both copolymers.

MALDI-TOF mass spectrometry confirmed the alternating order of the repeat units and provided insight into the identity of the polymer end-groups. For instance, the mass spectrum of **P3HTCp** exhibits two peak sets (Figure 2, top) with maximum intensities at *ca.* $m/z = 1194.96$ and 1068.93 amu respectively. The former (belonging to the major set) is consistent with a chain comprised of three pairs of alternating repeat units that are end-capped with 3-hexylthiophene-5-boronic acid pinacol esters, and extends to 3260.89 amu



Scheme 1 Synthesis of copolymers **PPCp**, **P3HTCp**, **PPT**, and **P3HTT**.

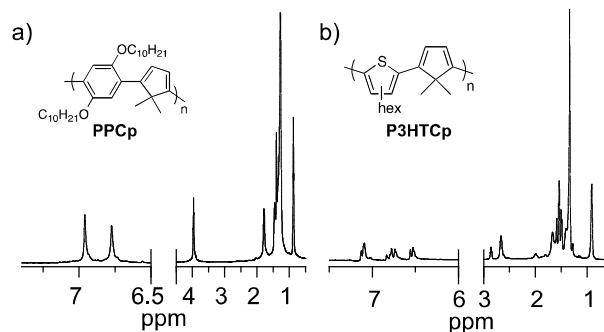


Fig. 1 ^1H NMR spectra (500 Mz, CD_2Cl_2) of a) **PPCp** and b) **P3HTCp**.

corresponding to a polymer comprised of 23 cyclic units. The alternate set of peaks of lower intensity are observed to be offset by *ca.* 126.04 amu, values that are consistent with the aforementioned structure absent a single 5-boronic acid pinacol ester group.

Similarly, the MALDI-TOF mass spectrum of **PPCp** (Figure 2, bottom) possesses a major peak set with a maximum intensity at *ca.* $m/z = 2203.25$ that is approximately the sum of four pairs of alternating repeat units, triflate and cyclopentadiene end groups, and a potassium ion; extending to *ca.* 4610.80 amu corresponding to a chain comprised of 19 cyclic units. The second peak set of lower intensity is offset by *ca.* $m/z = 92.06$ amu indicating that homocoupling between two cyclopentadiene monomers may have occurred. Indeed, the ^1H NMR and MALDI-TOF spectra of polyaromatic congeners **PPT** (Figures S6 and S9) and **P3HTT** (Figures S8 and S10) also reflect their proposed structures lending legitimacy to the comparative analyses to be discussed in subsequent sections of this study.

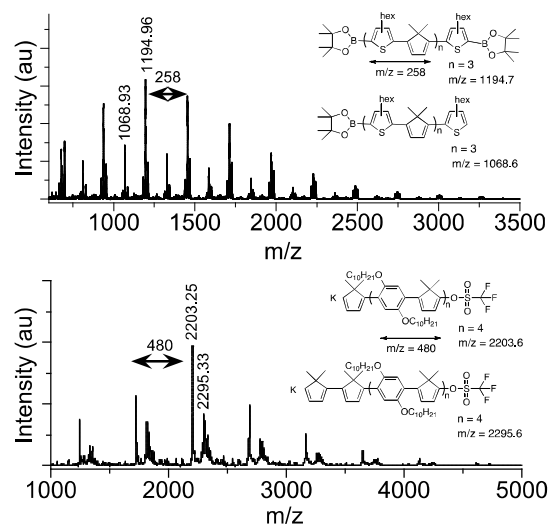


Fig. 2 MALDI-TOF mass spectra of **P3HTCp** (top) and **PPCp** (bottom).

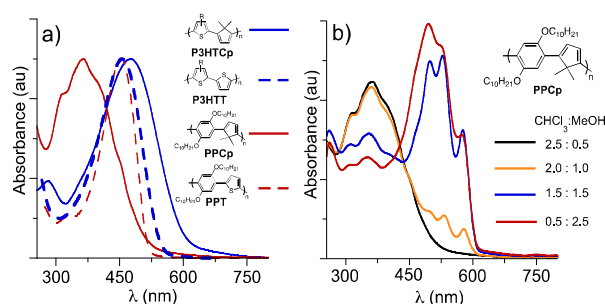


Fig. 3 (a) UV/vis absorption spectra of **P3HTCp**, **P3HTT**, **PPCp**, and **PPT** (in CH_2Cl_2). (b) UV/vis absorption spectra of **PPCp** on $\text{CHCl}_3/\text{MeOH}$ solvent mixtures. $R = \text{C}_6\text{H}_{13}$

UV/vis Absorption and Fluorescence Spectroscopy

All copolymer UV-vis absorption spectra were recorded in DCM (Figure 3a, Table 1) and exhibit absorption maxima for **P3HTT** ($\lambda_{\text{max}} = 457 \text{ nm}$), **PPT** ($\lambda_{\text{max}} = 454 \text{ nm}$), and **PFT** ($\lambda_{\text{max}} = 424 \text{ nm}$) that are in line with reported systems of comparable molecular structure (e.g., regiorandom poly(4-octyl-2,2'-bi(thiophene)), $\lambda_{\text{max}} = 458 \text{ nm}$;¹⁵ poly(1,4-(2,5-dihexadecyloxyphenylene)-2,5-thiophene), $\lambda_{\text{max}} \text{ ca. } 460 \text{ nm}$;¹⁶ and poly[2,5-(thienylene)-2,7-(9,9-dioctylfluorene)], $\lambda_{\text{max}} = 438 \text{ nm}$).¹⁷ The results also show an ipsochromic shift in both onset absorption λ_{onset} and λ_{max} (Table 1) when comparing the poly(3-hexylthiophene) and poly(flourene) derivatives **P3HTT** and **PFT** against **P3HTCp** and **PFCp** respectively, indicating a general reduction in optical band gap when diene constituents are used in lieu of thiophenes. Only among the poly(phenylene) derivatives is this trend reversed with **PPCp** exhibiting a λ_{onset} and λ_{max} (ca. 505 and 356 nm) that are blue shifted by ca. 11 and 89 nm respectively compared to **PPT**. Moreover, the poly(phenylene) derivatives are the only systems to exhibit solvatochromism. Indeed, absorption studies on **PPT** (Figure S11) using solvent mixtures of chloroform (as a good solvent) and methanol (as a poor solvent) show a reduction in λ_{max} (ca. 454 nm) that is accompanied by the growth of a low-energy shoulder at ca. 507 nm upon increasing the $\text{CHCl}_3/\text{MeOH}$ ratio (e.g. from 2.5:0.5 to 0.5:2.5). Comparatively, the electronic structure of **PPCp** is much more sensitive to solvent composition as made evident by the more pronounced shift in λ_{max} (from ca. 360 to 494 nm, Figure 3b) under identical conditions and the formation of well-defined vibronic fine structures that are consistent with a rigid and coplanar polymer backbone.¹⁸ This property has also been observed by Leclerc and coworkers in their investigations into the optical properties of structurally comparable poly(1,4-(2,5-dioctyloxyphenylene)-2,5-thiophene),¹⁹ and has been attributed to the modest energy barrier against coplanarity that is overcome by solvent interactions prompting inter-chain (e.g., aggregation) and/or intra-chain (e.g., chain-folding) mechanisms that enhance conjugation. On this basis, a more extensive bathochromic shift upon increasing $\text{CHCl}_3/\text{MeOH}$ ratios could be anticipated with **PPCp** given the greater steric demand of the geminal dimethyl groups that would impede coplanar conformations in

good solvents, a feature that may also explain why the $^1\text{H-NMR}$ chemical shift of the aromatic **PPCp** proton is positioned upfield from that observed from **PPT**. However, it should be noted that recent studies reported by Pozzo and coworkers²⁰ show no clear correlation between the optical properties of poly(3-alkylthiophene)s and polymer conformation. Consequently, additional efforts are required to determine the origin of these solvatochromic effects.

Fluorescence studies were performed and the results illustrated in Figures S12-15. All copolymers exhibit excitation spectra that are consistent with their optical absorption spectra with the exception of **PPCp** that exhibits an excitation maximum ($\lambda_{\text{exc}} = \text{ca. } 459 \text{ nm}$) that coincides with the low-energy shoulder in its UV/vis absorption spectrum. Regarding photoluminescence, the emission maximum λ_{em} of **PFT** (ca. 470 nm, $\Phi_{\text{F}} = 28 \pm 2\%$), **PPT** (ca. 517 nm, $\Phi_{\text{F}} = 48 \pm 7\%$), and **P3HTT** (ca. 564 nm, $\Phi_{\text{F}} = 35 \pm 7\%$) are blue shifted compared to **PFCp** (ca. 504 nm, $\Phi_{\text{F}} = 15 \pm 1\%$), **PPCp** (ca. 550 nm, $\Phi_{\text{F}} = 18 \pm 4\%$), and **P3HTCp** (ca. 600 nm, $\Phi_{\text{F}} = 5 \pm 3\%$) respectively. Perhaps more importantly, the polyaromatics possess higher quantum yields than their diene-containing congeners suggesting that the 4π electron moiety has an overall effect of compromising photoluminescence in these systems.

Table 1. Copolymer Characterization

	M_n^a	D_M	$\lambda_{\text{onset}}^b, \lambda_{\text{max}}^c$	E_{onset}^d	T_{dec}^e	T_g^f
PFCp	6.9	2.1	510, 452	0.79	200	98
PFT	6.0	1.3	475, 424	1.02	400	95
PPCp	9.1	2.5	505, 365	0.61	212	58
PPT	4.4	1.3	516, 454	0.66	404	54
P3HTCp	3.2	1.7	593, 476	0.42	190	36
P3HTT	2.3	1.4	542, 457	0.56	200	57

^a Determined by GPC (relative to poly(styrene) in THF, kg/mol). ^b UV/vis absorption onset (nm) in DCM. ^c UV/vis absorption maximum (nm) in DCM. ^d Onset of oxidation (V vs $\text{FeCp}^*_{2-}/\text{FeCp}^*_{2+}$, 0.1 M TBAPF₆ in DCM). ^e Decomposition temperature (°C), onset, determined by TGA. ^f Glass transition temperature (°C), second heating curve determined by DSC.

Thermal Properties

Thermal decomposition was analysed by TGA, revealing a two-step decomposition process (Figures S16-18) for all but copolymers **PFT** and **PPT** that degrade through a single step. The thermal decomposition temperature (T_{dec}) of each sample was recorded as the onset of mass loss with the data listed in Table 1. In sum, the poly(flourene) and poly(phenylene) derivatives are the most thermally stable (e.g. $T_{\text{dec}} > \text{ca. } 200^\circ\text{C}$) with the polyaromatics possessing a much higher T_{dec} within their copolymer class. Since glass transition temperature T_g can be of particular importance in assessing the processability and performance of a polymeric material, differential scanning calorimetry (DSC) was used to probe polymer thermal transitions as a function of constituent repeat unit. In contrast to thermal stability, differential thermograms (Figure S19-21) show similar features with T_g values comparable among the thiophene and diene congeners indicating that the identity of

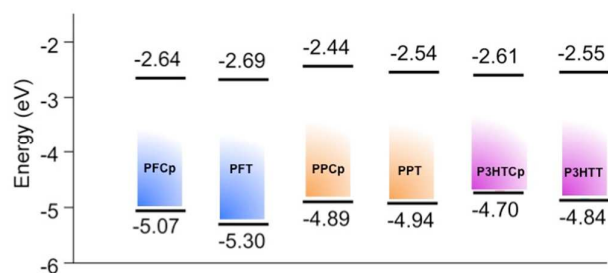


Fig. 4 Energy level diagram showing the estimated HOMO/LUMO levels of the poly(fluorene), poly(phenylene), and poly(3-hexylthiophene) derivatives calculated from CV and UV/vis absorption data.

the alternating repeat unit (e.g. 5,5-dimethylcyclopentadiene vs thiophene) has a modest effect on the glass transition.

(Spectro)electrochemistry

Onset oxidation potentials (E_{onset}) were measured from cyclic voltammograms (Figures S22-27) and reported with respect to the decamethylferrocene redox couple $[\text{FcCp}^*]^{+/0}$. Consistent among all copolymers was a reduction in E_{onset} (Table 1) in the order of poly(fluorene), poly(phenylene), and poly(3-hexylthiophene) derivatives suggesting that the aromatic co-repeat unit plays a critical role in establishing the HOMO level energy among these systems. Moreover, when the congeners are compared against each other, E_{onset} of the diene-containing systems are consistently lower indicating that the cyclic diene scaffolds increase the copolymer HOMO level when used in lieu of thiophenes, results that are illustrated in the HOMO-LUMO energy diagrams in Figure 4 estimated from CV and UV/vis spectroscopic data.

Spectroelectrochemical analysis (Figures 5a-d) on drop-casted copolymer films deposited on ITO were examined to gain insight into charge-carrier evolution during oxidation in 0.1 M TBAPF₆/MeCN solutions. Consistent with data acquired in the solution-phase, neutral films of **PFCp** and **PPT** exhibit absorption maxima (i.e., λ_{max} = 444 and 457 nm respectively) that are red shifted to those of **PFT** and **PPCp** respectively (i.e., **PFT**, λ_{max} = 415 nm; **PPCp**, λ_{max} = 400 nm). The stepwise oxidation of **PFCp** (Figure 5a) results in the generation of two major low-energy polaronic bands at 700 and 1069 nm that is accompanied by a bleaching of the neutral-state λ_{max} . Under similar oxidizing conditions, the energy difference between the absorption maxima of the two major **PFT** charge-carrier bands (Figure 5c) appear to be much larger with the higher energy band (λ_{max} = 590 nm) blue-shifted from its comparable in **PFCp** and lower energy band extending well into the near IR region of the electromagnetic spectrum. Indeed, these features are also observed when comparing the spectroelectrochemical profiles of poly(phenylene) derivatives **PPT** and **PPCp** (Figures 5b and d) indicating that the 5,5-dimethylcyclopentadiene moieties significantly impact the electronic structure of the copolymer in the oxidized state. Unfortunately, comparisons between the poly(3-hexylthiophene) derivatives were not possible due to the solubility of the **P3HTCp** films in MeCN

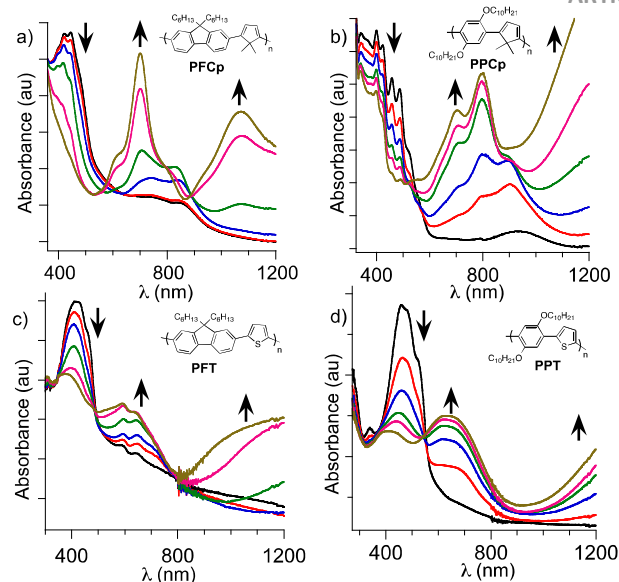


Fig. 5 Spectroelectrochemical profiles of: a) **PFCp**, b) **PPCp**, c) **PFT**, and d) **PPT** held between ca. 0.95-1.15 V, 0.90-1.10 V, 1.20-1.40 V, and 0.75-0.95 V (vs. Ag/Ag^+), respectively. All black UV/vis/NIR spectra were taken from films in their neutral state. All subsequent spectra (i.e., red, blue, green, pink, and brown) were taken at progressively higher potentials at 50 mV intervals over the ranged indicated above.

upon oxidative doping. However, data obtained from **P3HTT** show spectral features (Figure S28) that are similar to those observed in electrochemically-generated poly(3-methylthiophene) films²¹ indicating that the charge-carrying species are similar in both systems.

Stability

All copolymers exhibit long-term environmental stability in the solid state as evidenced by the virtually identical ¹H NMR and GPC traces taken over a period ca. 6 months. On the contrary, the very same copolymers were observed to degrade in solution under ambient conditions, prompting us to examine their stability in DCM by plotting the percent ratio of λ_{max} absorbance (A) at time t and 0 (i.e. $A_t/A_0 \times 100\%$) versus t . To account for the variability of the copolymer molar absorptivities, stock solutions were prepared within a concentration range where the Beer-Lambert law was applicable. The contents of each stock solution were then

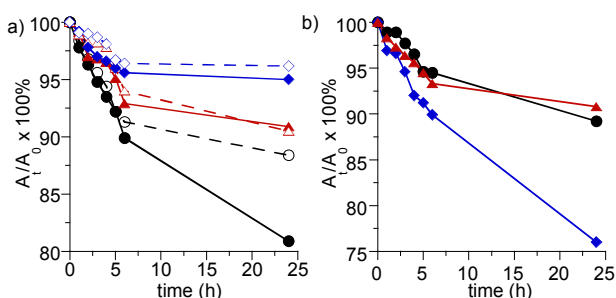


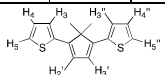
Fig. 6 Percent ratio of λ_{max} absorbance (A) at time t and 0 (i.e. $A_t/A_0 \times 100\%$) versus t for: a) copolymers **PFCp** (●, black solid), **PFT** (○, black dash), **PPCp** (▲, red solid), **PPT** (△, red dash), **P3HTCp** (◆, blue solid), **P3HTT** (◇, blue dash), and b) model triads **3** (●, black solid), **4** (●, black solid), and **5** (▲, red solid).

dispensed into volumetric flasks left exposed to air and light under ambient conditions. Over the course of several hours, a new flask was selected at random and its contents placed in a UV/vis absorption spectrometer for analysis. In sum, the results (Figure 6a) reveal the poly(3-hexylthiophene) derivatives to be the most stable in solution among the three copolymer classes, with the poly(fluorene) derivatives exhibiting the largest degree of decomposition over an identical period. Moreover, the stability of the cyclopentadiene-containing copolymers are comparable to their thiophene-containing congeners with the exception of **PFCp** which loses *ca.* 20% of its original optical absorbance compared to **PFT** losing *ca.* 12 % over the same 24 h period. Taken together, the data indicate that care should be taken when handling these copolymers in solution and that there is no clear trend relating the identity of the comonomer structure (5,5-dimethylcyclopentadiene vs thiophene) and stability among these systems under the conditions studied here.

Table 2 ^1H NMR Chemical Shifts^a of the Aromatic Region of Model Triads of **P3HTCp**.

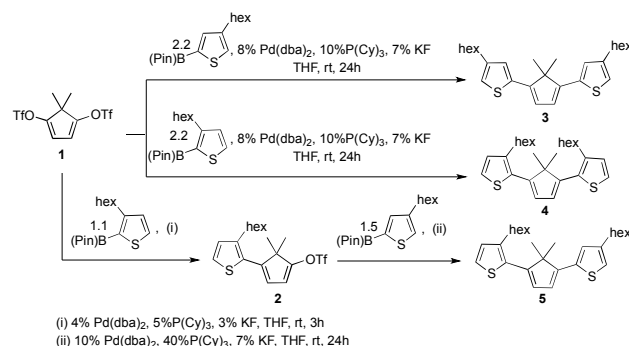
3 (T-T)	H5	H3	H2'	H3'	H3''	H5''
	6.80	7.01	6.65	6.65	7.01	6.80
4 (H-H)	H5	H4	H2'	H3'	H4''	H5''
	7.25	7.01	6.46	6.46	7.01	7.25
5 (H-T)	H5	H4	H2'	H3'	H3''	H5''
	7.25	7.01	6.41	6.69	7.01	6.81

^a δ in ppm (CD_2Cl_2)



P3HTCp Regiochemistry

Since regiochemistry can govern the optical and electronic properties of π -conjugated polymers by way of influencing conformation between adjacent units (and therefore the degree of conjugation), we were compelled to gain insight into the regiochemistry of **P3HTCp** by examining the spectral pattern of the olefinic protons. Towards this end, model triads **3-5** were prepared according to Scheme 2, representing all modes by which the central 5,5-dimethylcyclopentadiene group can be α,α' -coupled to two 3HT units via the 1- and 4-positions (*i.e.* spaced in a head-to-tail (H-T), tail-to-tail (T-T), or



Scheme 2 Synthesis of P3HTCp model triads **3-5**.

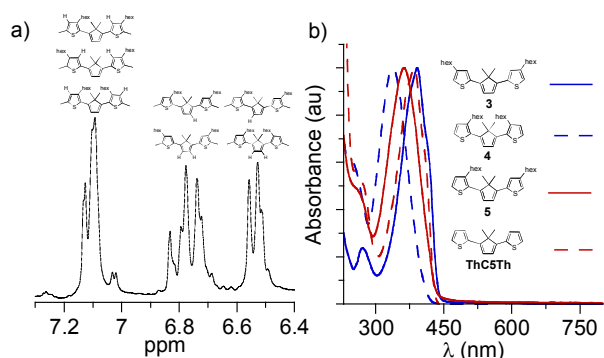


Fig. 7 a) ^1H NMR spectrum (500 Mz, CD_2Cl_2) of aromatic region of **P3HTCp**. b) UV/vis absorption spectra of ThC5Th and **3-5** (in CH_2Cl_2).

head-to-head (H-H) arrangement). With the aid of heteronuclear single quantum coherence (HSQC) and heteronuclear multiple bond coherence (HMBC) NMR spectroscopy (see Figures S29-34 for related spectra), peak assignments were made based on proton chemical shifts in the aromatic region that are listed in Table 2. Notably, the chemical shift order and variation between the 3HT H3(4,5) and H3''(4'',5'') peaks are near identical to those of the P3HT model triads reported by Barbarella and coworkers.²² Moreover, the tabulated data show that the 3HT H3'' and H4'' protons resonate at approximately the same frequency (*i.e.* 7.01 ppm) regardless of regiochemistry, while the olefinic protons resonate at *ca.* δ 6.65-6.69 and 6.41-6.46 ppm when adjacent to 3HT tail and head ends respectively. Indeed, the aromatic region of the **P3HTCp** ^1H NMR spectrum (Figure 7a) consists of three distinct peak sets centered at 7.15, 6.82, and 6.57 ppm accounting for a relative signal integration of 1.0, 1.2, and 0.8. The constancy of these three sets of signals in the aromatic region, along with those of the latter that are deshielded by *ca.* 0.13-0.17 ppm with respect to the protons of **3-5** suggests that the assignment of the **P3HTCp** peaks follow the same order as that observed for the triads. In sum, the peaks centered at 6.57 and 6.82 ppm are attributed to the olefinic protons having H-H/H-T and T-T/H-T junctions respectively, with the peaks centered at 7.15 ppm attributed to the aromatic 3HT protons indicating a regiorandom polymeric backbone.

The UV/vis absorption spectra of model triads **3-5** are shown in Figure 7b along with ThC5Th bearing unsubstituted thiophene units for comparison. Consistent with the trend observed among P3HT model triads,²² the λ_{max} of **3-5** (*ca.* λ_{max} = 392, 337, and 363 nm respectively) decrease in the order of increasing H-H junctions. This can be attributed to steric congestion between hexyl and dimethyl groups of the thiophene and diene moieties respectively that twist adjacent rings out of plane and reduce π -conjugation. This would also explain why: i) compounds **4** and **5** exhibit a λ_{max} that is ipsochromically shifted to that of ThC5Th, despite a bathochromic effect that should be exerted by the hexyl groups as observed in **3** and ii) the relatively low stability of **3** (Figure 6b) that likely arises from its ability to adopt coplanar

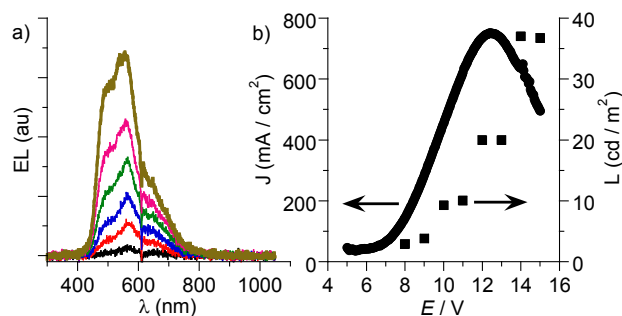


Fig. 8 a) Electroluminescence (EL) spectra are from a PLED with the general device structure ITO/PEDOT:PSS/PFCp/Alq₃/Al taken at 7 V (black), 8 V (red), 9 V (blue), 10 V (green), 11 V (pink), and 12 V (brown). b) Current density-voltage-luminescence (J-V-L) curves for PFCp-based PLED.

conformations more readily making it susceptible to oxidative degradation.

Polymer Light-Emitting Diode

Poly(dialkylfluorene)s and related derivatives have been studied extensively as emissive layers in polymer light-emitting diodes (PLEDs) due to their electroluminescence (EL) capabilities, oxidative and thermal stability, and solubility in common organic solvents.²³ Inspired by the potential of this polymer class, a PFCp-based PLED was constructed with a device architecture of ITO/PEDOT:PSS/PFCp/Alq₃/Al to determine whether the alternating cyclopentadienyl repeat units compromise electroluminescence in this form of a poly(fluorene) derivative. Indeed, Figure 8a shows the EL ($\lambda_{em} = 556$ nm) of this device that is comparable to the photoluminescence (PL) measured from a PFCp film deposited on ITO⁸ and red shifted to the EL of a poly(9,9-dihexylfluorene) PF- and PFT-based device (EL $\lambda_{em} = 450$ and 515 nm respectively) reported by Carter and coworkers.²⁴ Moreover, the J-V-L curve in Figure 8b indicates that PFCp exhibits relatively weak electroluminescence even at relatively high bias of ca. 12 V suggesting that device optimization is required. Nonetheless, this is to the best of our knowledge, the first example of any kind of PLED employing a cyclopentadiene-based polymer as an active layer, providing a proof-of-principle that copolymers of this type can be fabricated into functioning (opto)electronic devices.

4. Summary and Conclusions

In summary, we report on a comparative analysis encompassing poly(fluorene), poly(phenylene), and poly(3-hexylthiophene) derivatives bearing alternating thiophene or 5,5-dimethylcyclopentadiene repeat units. The results of our findings show that optical absorption, photoluminescence, HOMO/LUMO energies, and charge-carrier generation are highly influenced by the identity of the co-repeat unit irrespective of copolymer class. While having a modest effect on glass transition temperature, supplanting thiophene constituents with diene alternatives lends thermal stability to the π -conjugated systems, however, all copolymers were

found to exhibit some decomposition in solution under ambient conditions. Given the asymmetry of the 3-hexylthiophene repeat unit, model triads of P3HTCp were prepared and characterized by HSQC and HMBC NMR spectroscopy to elucidate regiochemistry that was determined to be regiorandom. Finally, a functioning PLED employing PFCp as an emissive layer was fabricated providing a proof-of-principle that polyene-like π -conjugated systems bearing 4 π electron 5,5-dimethylcyclopentadiene constituents can be employed as active layers in optoelectronic devices. On the basis of the results reported here, future efforts will focus on the design and synthesis of polyene-like (macro)molecules with reduced aromatic character that we envision will lead to the realization of π -conjugated systems with enhanced optical and electronic properties.

Acknowledgements

The authors thank Rutgers University for financial support and the NSF for funds used to purchase the Bruker ASCEND 500 MHz spectrometer (NSF MRI 1229030).

1

¹ (a) M. Leclerc and K. Faïd, *Adv. Mater.* 1997, **9**, 1087-1094. (b) J. G. C. Veinot and T. J. Marks, *Acc. Chem. Res.* 2005, **38**, 632-643. (c) M. Jeffries-El, G. Sauve, and R. D. McCullough, *Macromolecules* 2005, **38**, 10346-10352. (d) P. M. Beaujuge and J. R. Reynolds, *Chem. Rev.* 2010, **110**, 268-320. (e) C. Friebe, M. D. Hager, A. Winter and U. S. Schubert, *Adv. Mater.* 2012, **24**, 332-345. (f) S. W. Thomas III, G. D. Joly and T. M. Swager, *Chem. Rev.* 2007, **107**, 1339-1386. (g) D. T. McQuade, A. E. Pullen and T. M. Swager, *Chem. Rev.* 2000, **100**, 2537-2574. (h) Y. -J. Cheng, S. -H. Yang and C. -S. Hsu, *Chem. Rev.* 2009, **109**, 5868-5923. (i) Handbook of Thiophene Based Materials (Eds: I. F. Perepichka, D. F. Perepichka), JohnWiley & Sons, Hoboken, NJ, USA 2009. (j) M. Scheuble, M. Goll and S. Ludwigs, *Macromol. Rapid Commun.* 2015, **36**, 115-137.

² J. Roncali, *Chem. Rev.* 1992, **92**, 711-738.

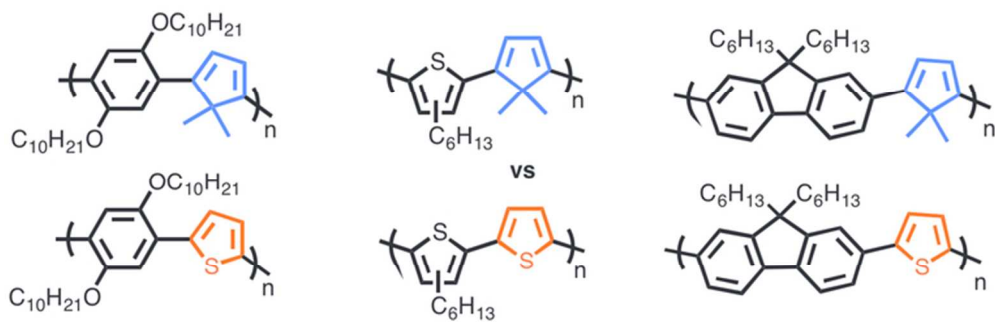
³ (a) S. Rozen and Y. Bareket, *J. Chem. Soc. Chem. Commun.* 1994, **17**, 1959-1960. (b) S. Rozen and Y. Bareket, *J. Org. Chem.* 1997, **62**, 1457-1462. (c) Y. Miyahara and T. Inazu, *Tetrahedron Lett.* 1990, **31**, 5955-5958. (d) M. M. Oliva, J. Casado, J. T. López Navarette, S. Patchkovskii, T. Goodson III, M. R. Harpham, J. S.

- Seixas de Melo, E. Amir and S. Rozen, *J. Am. Chem. Soc.* 2010, **132**, 6231-6242. (e) C. Zhang, T. H. Nguyen, J. Sun, R. Li, S. Black, C. E. Bonner and S. -S. Sun, *Macromolecules* 2009, **42**, 663-670. (f) S. M. King, I. I. Perepichka, I. F. Perepichka, M. R. Bryce and L. -O. Pålsson, *Chem. Commun.* 2005, **27**, 3397-3399. (g) S. Beaupré and M. Leclerc, *Adv. Funct. Mater.* 2002, **12**, 192-196. (h) G. Barbarella, O. Pudova, C. Arbizzani, M. Mastragostino and A. Bongini, *J. Org. Chem.* 1998, **63**, 1742-1745. (i) G. Barbarella, L. Favaretto, M. Zambianchi, O. Pudova, C. Arbizzani, A. Bongini and M. Mastragostino, *Adv. Mater.* 1998, **10**, 551-554. (j) E. Amir and S. Rozen, *Angew. Chem. Int. Ed.* 2005, **44**, 7374-7378.
- ⁴ (a) E. Amir, K. Sivanandan, J. E. Cochran, J. J. Cowart, S. -Y. Ku, J. H. Seo, M. L. Chabinyk and C. J. Hawker, *J. Polym. Sci., Part A: Polym. Chem.* 2011, **49**, 1933-1941. (b) S. Wei, J. Xia, E. J. Dell, Y. Jiang, R. Song, H. Lee, P. Rodenbough, A. L. Briseno, and L. M. Campos, *Angew. Chem., Int. Ed.* 2014, **53**, 1832-1836. (c) C. -H. Tsai, D. N. Chirdon, A. B. Maurer, S. Bernhard and K. J. T. Noonan, *Org. Lett.* 2013, **15**, 5230-5233 .
- ⁵ (a) N. Camaioni, G. Ridolfi, V. Fattori, L. Favaretto and G. Barbarella, *Appl. Phys. Lett.* 2004, **84**, 1901-1903. (b) E. J. Dell and L. M. Campos, *J. Mater. Chem.* 2012, **22**, 12945-12952.
- ⁶ E. Busby, J. Xia, Q. Wu, J. Z. Low, R. Song, J. R. Miller, X. Y. Zhu, L. M. Campos and M. Y. Sfeir, *Nat. Mater.* 2015, 426-433.
- ⁷ (a) J. Roncali, *Macromol. Rapid. Commun.* 2007, **28**, 1761-1775. (b) J. D. Azoulay, Z. A. Koretz, B. M. Wong and G. C. Bazan, *Macromolecules* 2013, **46**, 1337-1342. (c) P. Coppo, D. C. Cupertino, S. G. Yeates and M. L. Turner, *Macromolecules* 2003, **36**, 2705-2711. (d) T. L. Lambert and J. P. Ferraris, *J. Chem. Soc., Chem. Commun.* 1991, 752-754. (e) J. P. Ferraris and T. L. Lambert, *J. Chem. Soc., Chem. Commun.* 1991, 1268-1270. (f) G. A. Elbaz, L. M. Repka, and J. D. Tovar, *ACS Appl. Mater. Interfaces*, 2011, **3**, 2551-2556. (g) P. A. Peart, and J. D. Tovar, *Org. Lett.* 2007, **9**, 3041-3044.
- ⁸ L. Chen, S. M. Mahmoud, X. Yin, R. A. Lalancette and A. Pietrangelo, *Org. Lett.* 2013, **15**, 5970-5973.
- ⁹ M. E. Vega, L. Chen, M. R. Khoshi, C. Casseus and A. Pietrangelo, *RSC Advances* 2015, **5**, 54727-54734.
- ¹⁰ W. Chen, H. Li, J. R. Widawsky, C. Appayee, L. Venkataraman and R. Breslow, *J. Am. Chem. Soc.* 2014, **136**, 918-920.
- ¹¹ K. C. Nicolaou, J. Hao, M. V. Reddy, P. B. Rao, G. Rassias, S. A. Snyder, X. Huang, D. Y. -K. Chen, W. E. Brenzovich, N. Giuseppone, P. Giannakakou and A. O'Brate, *J. Am. Chem. Soc.* 2004, **126**, 10174-10182.
- ¹² J. C. Li, H. Y. Lee, S. H. Lee, K. Zong, S. H. Jin and Y. S. Lee, *Synth. Met.* 2009, **159**, 201-208.
- ¹³ M. Manceau, E. Bundgaard, J. E. Carle, O. Hagemann, M. Helgesen, R. Søndergaard, M. Jørgensen and F. C. Krebs, *J. Mater. Chem.* 2011, **21**, 4132-4141.
- ¹⁴ (a) J. Sakamoto, M. Rehahn, G. Wegner and A. D. Schlüter, *Macromol. Rapid Commun.* 2009, **30**, 653-687. (b) J. P. Corbet and G. Mignani, *Chemical Reviews* 2006, **106**, 2651-2710.
- ¹⁵ J. P. Lère-Porte, J. J. E. Mreau and C. Torrelles, *Eur. J. Org. Chem.* 2001, 1249-1258.
- ¹⁶ Z. Bao, W. Chan and L. Yu, *Chem. Mater.* 1993, **5**, 2-3.
- ¹⁷ A. D. Bouillud, I. Lévesque, Y. Tao and M. D'lorio, *Chem. Mater.* 2000, **12**, 1931-1936.
- ¹⁸ J. -M. Raimundo, P. Blanchard, N. Gallego-Planas, N. Mercier, I. Ledoux-Rak, R. Hierle and J. Roncali, *J. Org. Chem.* 2002, **67**, 205-218.
- ¹⁹ G. Duresne, J. Bouchard, M. Belletête, G. Durocher and M. Leclerc, *Macromolecules* 2000, **33**, 8252-8257.
- ²⁰ G. M. Newbloom, S. M. Hoffmann, A. F. West, M. C. Gile, P. Sista, H. -K. Cheung, C. K. Luscombe, J. Pfaendtner and L. D. Pozzo, *Langmuir* 2015, **31**, 458-468.
- ²¹ S. Alkan, C. A. Cutler and J. R. Reynolds, *Adv. Funct. Mater.* 2003, **13**, 331-336.

²² G. Barbarella, A. Bongini and M. Zambianchi, *Macromolecules* 1994, **27**,3040-3045.

²³ (a) B. Nowacki, E. Imazaki, A. Cirpan, F. Karasz, T. D. Z. Atvars and L. Akcelrund, *Polymer* 2009, **50**, 6057-6064. (b) B. Liu and W. Huang, *Thin Solid Films* 2002, **41**, 206-210. (c) M. Gaal, J. W. List and U. Scherf, *Macromolecules* 2003, **36**, 4236-4237. (d) N. M. Cho, D. -H. Hwang, J. -I, Lee, B. -J. Jung and H. -K. Shim, *Macromolecules* 2002, **35**, 1224-1228. (e) Q. Pei and Y. Yang, *J. Am. Chem. Soc.* 1996, **118**,7416-7417.

²⁴ A. R. Davis, J. J. Peterson and K. K. Carter, *ACS Macro Lett.* 2012, **1**, 469-472.



Comparative Analyses: • optical absorption • T_g • (spectro)electrochemistry
 • photoluminescence • T_{dec} • solution-phase stability

64x28mm (300 x 300 DPI)